ELSEVIER

Journal of Molecular Structure (Theochem) 571 (2001) 7–26

THEO CHEM

www.elsevier.com/locate/theochem

Conformational potential energy surfaces of a Lycopene model

Gregory A. Chasse[a,b,*], Kenneth P. Chasse[a], Arpad Kucsman[c], Ladislaus L. Torday[d], Julius G. Papp[d]

[a]*Velocet Communications Inc., 210 Dundas St. W., Suite 800 Toronto, Ont., Canada M5G 2E8*
[b]*Department of Chemistry, University of Toronto, Toronto, Ont., Canada M5S 3H6*
[c]*Department of Organic Chemistry, Eötvös Loránd University of Budapest, P.O. Box 32, H-1518 Budapest 112, Hungary*
[d]*Department of Pharmacology and Pharmacotherapy, Albert Szent-Gyorgy Medical University, H-6701 Szeged, Hungary*

Received 30 October 2000; accepted 5 February 2001

Abstract

Ab initio conformational analysis has been carried out at the RHF/3-21G level of theory. Computations were performed on a tail-end lycopene (Model B). Both the all-*trans* and the 5-*cis*-isomers were studied. The fully planar structure turned out to be a second-order saddle point, which indicated that lycopene itself is not planar. Most of the conformers of the 5-*cis*-isomer are more stable than the corresponding conformers of the all-*trans*-isomer. This stability is in agreement with the observation that even though lycopene is biosynthesized in plants as the all-*trans* form, in the human body over 65% exists in one of the *cis*-forms and less than 35% remains in its all-*trans* form. © 2001 Elsevier Science B.V. All rights reserved.

Keywords: Conformational analysis; All *trans*-lycopene tail-end model; Selected *cis*-isomers of lycopene tail-end model; Conformational potential energy surfaces; 2D scans; Ab initio MO theory

1. Introduction

1.1. Biological background

Several chronic diseases, amongst which are cancer and cardiovascular diseases, are related to oxidative stress which is now recognized as an important etiological factor. Antioxidants are effective in reducing the damaging effect of oxygen containing radicals and radicaloids such as $^{\cdot}OH$, O_2^{-}, H_2O_2 as well as that of singlet oxygen $^1O_2$. Lycopene is a carotenoid type antioxidant, present in tomatoes and other fruits and vegetables. Studies have shown that lycopene acts as an antioxidant in vivo, providing protection against the oxidation of lipids, proteins and DNA [1,2]. A recently published review [3] indicated a significant inverse correlation between the intake of lycopene and therefore the serum concentrations of lycopene and the risk of several diseases including cancer. In the absorption and bio-availability the isomeric forms of lycopene appear to play an important role.

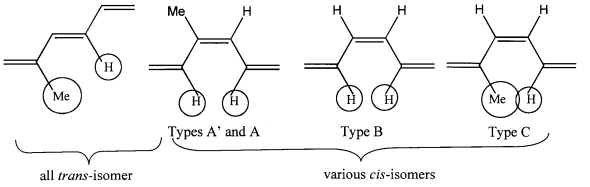

Scheme 1.

* Corresponding author. Address: Velocet Communications Inc., 210 Dundas St. W., Suite 800 Toronto, Ont., Canada M5G 2E8. Tel.: +1-416-978-3598; fax: +1-416-978-3598.
E-mail address: gchasse@fixy.org (G.A. Chasse).

PII: S0166-1280(01)00413-4

1.2. Structural background

The skeleton of lycopene [$C_{40}H_{56}$] consists of eight isoprenic units, thus, it is related to tetraterpenes [$C_{40}H_{64}$] even though it contains fewer hydrogens and therefore more double bonds. Its composition is shown in **I** in its fully extended form which is the all *trans*-lycopene. As such, lycopene is closely related to β-carotenes.

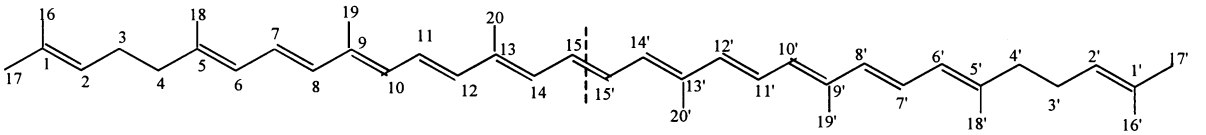

I

Sometimes, the structure of lycopene is presented in a pre-folded form (**II**) to show its structural similarity to β-carotene. Due to the internal molecular symmetry, it has been traditional to number the chain from the two ends as shown in **I** and **II**.

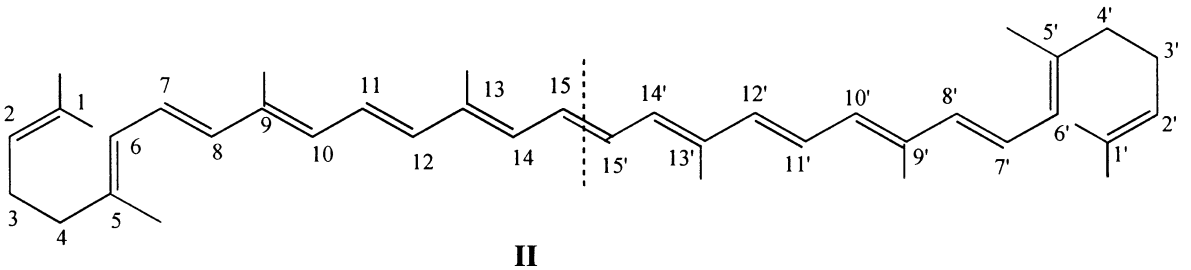

II

The history of lycopene [1–14] reveals an interesting story from the initial curiosity of a colourful substance in the 1910s to the medical application in the 1990s as an antioxidant.

In 1943, Pauling pointed out [14] not all *cis*-isomers may be of equal stability due to a number of possible 1,4 interactions as shown by the following structures. Clearly, on the basis of relative group sizes, the –CH_3–H– interaction (type C) appears to be the most destabilizing (Scheme 1).

No X-ray structure of lycopene has been determined as yet. There are, however, two X-ray structures of β-carotene in the literature [15,16].

1.3. Computational background

In fruits and vegetables Lycopene is present mostly in its all-*trans* isomeric form. However, *cis*-isomers constitute the predominant form present in the serum and tissues [17,18]. This observation suggests that at least some of the *cis*-isomers may be energetically comparable to the stability of the all-*trans* isomers. Fig. 1 shows the all-*trans*- and selected *cis*-isomers of lycopene. The all-*trans*- and the selected six *cis*-isomers (5-, 7-, 9-, 11-, 13- and 15-) are yet to be explored computationally in their molecular

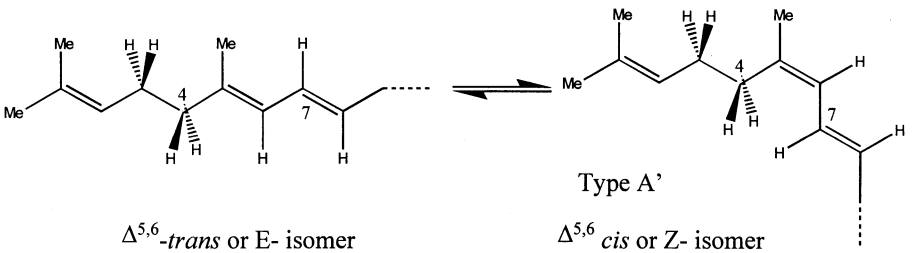

Scheme 2.

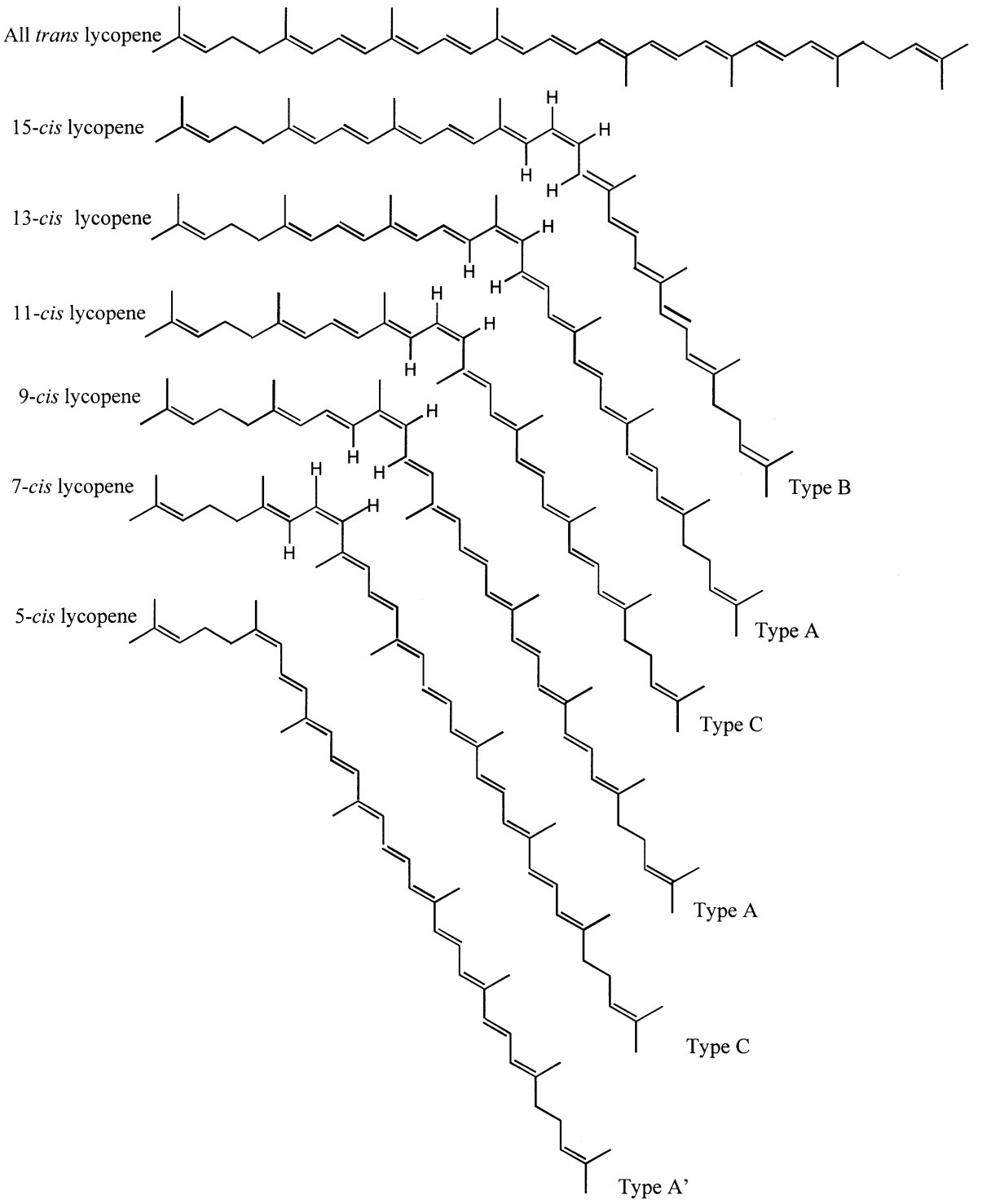

Fig. 1. Geometrical isomers of lycopene.

entirety (containing 296 electrons and 96 atoms, which corresponds to 282 geometrical parameters to be optimized). Thus, lycopene may well be among the largest organic molecules to be investigated, using ab initio molecular computation, with the current computational technology. The relative energies for the four types of structures, are depicted in Fig. 1, are expected to exhibit four categories of stability. Consequently, we may anticipate four energy ranges.

Type A′ involves the 5-*cis*-isomer.
Type A involves the 9-*cis* and 13-*cis*-isomers.
Type B involves the 15-*cis*-isomer.
Type C involves the 7- and 11-*cis*-isomers.

Type A′ is extremely similar to Type A (see Fig. 1) except that the hydrogens, involved in 1,4 interactions (attached to carbons 4 and 7), are not eclipsed but staggered. This is illustrated in greater detail by Scheme 2.

2. Scope

The presence of three consecutive carbon–carbon single bonds (C^2–C^3–C^4–C^5) suggests conformational flexibility of the tail-ends of lycopene. It was deemed desirable therefore to study the conformational intricacy of the tail-end of lycopene by choosing some model compound. If one looks at the lycopene structure, one can cut out from the full molecule shorter segments and terminate them with hydrogen atoms. These model compounds are labelled in Scheme 3 as Model A, Model B, Model C, Model D, etc.

For the present study, we have chosen Model B in order to be able to mimic conformationally, the tail-end of the all-*trans* isomer, as well as the 5-*cis* isomer, as depicted in Scheme 4.

3. Method

In order to learn about the conformational behaviours of the two tail-end conformations of lycopene, Model B (**III**) was studied in more detail. This truncated lycopene model (C^1–C^8 segment) contains of the first three double bonds of lycopene. Structure **III** shows the fully extended form of Model B.

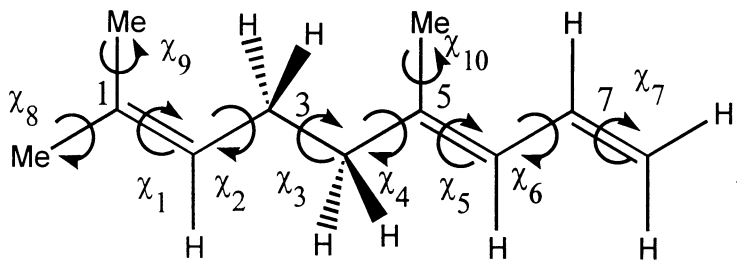

χ_1: Me-C^1-C^2-C^3
χ_2: C^1-C^2-C^3-C^4
χ_3: C^2-C^3-C^4-C^5
χ_4: C^3-C^4-C^5-C^6
χ_5: C^4-C^5-C^6-C^7
χ_6: C^5-C^6-C^7-C^8
χ_7: C^6-C^7-C^8-H

III

When a planar moiety is rotated about a tetrahedral carbon, it may be either eclipsed with a tetrahedral bond or perpendicular to that bond. This has been revealed by the study on ethyl benzene [19]. These idealized conformers are illustrated by Scheme 5.

Single scans can be carried out to study the rotation about the C^2–C^3(χ_2), C^3–C^4(χ_3) and C^4–C^5(χ_4) single bonds of **III**. However, the conformational problem is better studied in the form of a potential energy hyper-surface (PEHS), which involves all three torsional angles.

$$E = f(\chi_2, \chi_3, \chi_4). \quad (1)$$

Since the rotation about the single C–C bond (χ_3) is expected to be in g^+, a, g^- configurations, therefore three potential energy surfaces (PES)

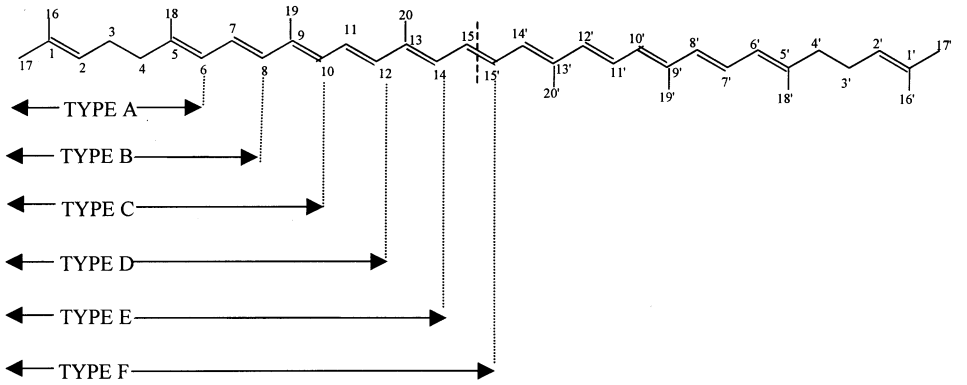

Scheme 3.

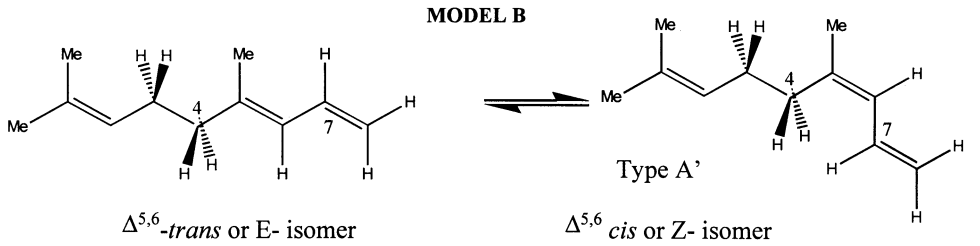

Scheme 4.

may be generated at these three orientations of χ_3.

$$E = f(\chi_2, \chi_4) \quad \text{at} \quad \chi_3 = +60°, \tag{2a}$$

$$E = f(\chi_2, \chi_4) \quad \text{at} \quad \chi_3 = +180°, \tag{2b}$$

$$E = f(\chi_2, \chi_4) \quad \text{at} \quad \chi_3 = +300°(-60°). \tag{2c}$$

The levels of these 2D cross-sections are shown in Fig. 2.

One may also generate 1D cross-sections such as

$$E = f(\chi_2) \quad \text{at} \quad \chi_3 = 180°, \quad \chi_4 = \pm 90°, \tag{3a}$$

$$E = f(\chi_3) \quad \text{at} \quad \chi_2 = \pm 90°, \quad \chi_4 = \pm 90°, \tag{3b}$$

$$E = f(\chi_4) \quad \text{at} \quad \chi_2 = \pm 90°, \quad \chi_3 = 180°. \tag{3c}$$

The location of these conformational potential

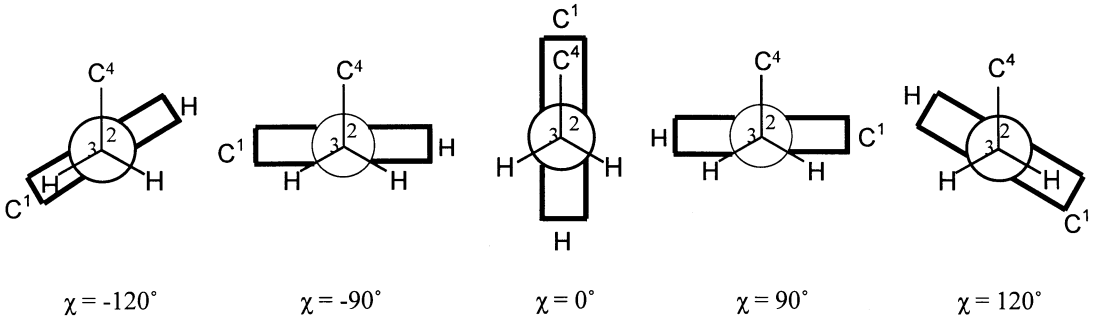

Scheme 5.

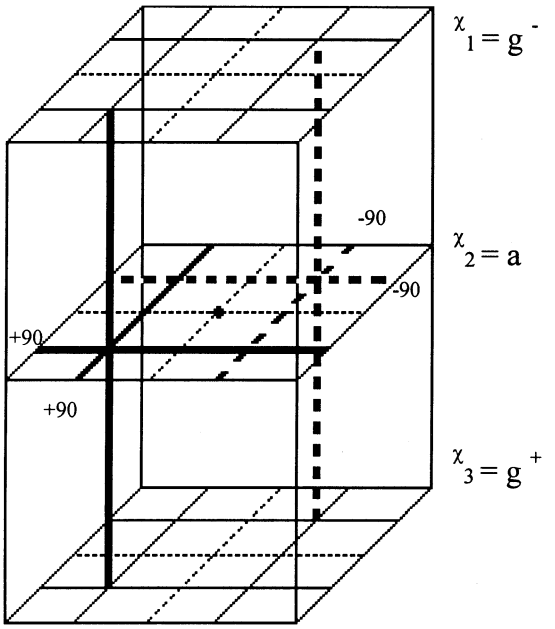

Fig. 2. A schematic representation of the conformational PEHS, $E = f(\chi_2, \chi_3, \chi_4)$ of lycopene Model B. The heavy dot, at the centre, illustrates the location of the fully symmetric conformation as drawn in **III**. The three levels indicate the three 2D cross-sections (PES) and the three perpendicular heavy broken and solid lines specify the locations of the three 1D cross-sections (PEC) investigated.

energy curves (PEC) are indicated by three heavy solid lines and three heavy broken lines in Fig. 2.

The computations were carried out using the GAUSSIAN 98 program system [20]. Standard geometry optimizations were performed on the all-*trans* as well as six selected *cis*-isomers.

4. Results and discussion

4.1. Molecular conformations

The conformational PEHS, as specified by Eq. (1), illustrated schematically in Fig. 2, is applicable for both the all-*trans*- and for the 5-*cis*-isomer of lycopene Model B (**III**).

4.1.1. The all-trans-structure

The all-*trans*-lycopene Model B (**III**) was subjected first to conformational analysis. The conformational PEHS (1) of three independent variables, was investigated in terms of three PESs (2) of two independent variables. These three PESs are depicted in landscape and contour representations in Figs. 3–5. For Fig. 3, χ_3 was kept in its *anti*-position (**2b**), for Fig. 4, χ_3 was kept in g^+ and for Fig. 5, χ_3 was kept in g^- position. Clearly the central level of Fig. 2, for which the PES (**2b**) is depicted in Fig. 3, is the most symmetric. By inspection, we may anticipate the presence of nine minima on the PES. These are listed in Scheme 6.

Those minima located at the edges are repeated twice and the structure at the corner is repeated four times. These repeated structures are shown in square brackets, leaving nine unique conformers (which are not in square brackets). Since there are three levels, as shown in Fig. 2, the three PESs (Figs. 3–5) may contain up to $3 \times 9 = 27$ stable conformations. The 1D scans leading to the three PECs (shown at the left-hand side of Fig. 6) indeed suggest the existence of three unique minima, on each of the three PECs. This reconfirms that $3^3 = 27$ minima may be anticipated. However, sometimes expected minima are annihilated from the PES. Geometry optimizations have been initiated on these 27 conformations.

The optimized torsional angles are summarized in Table 1. Indeed a few minima, involving some *syn*-orientations, were annihilated. The torsions about the single bonds (χ_2, χ_3 and χ_4) are shown in bold. Al other torsional angles are associated with double bonds. Since this is the all-*trans* form, these double bonds should have dihedral angles in the vicinity of $\pm 180°$. The last double bond, however, is ending in CH_2, so one of the two hydrogens are *trans* (χ_7) and the other is *cis*. In Table 1, the last three dihedral

[s(a)s]	**[g^+(a)s]**	**[g^-(a)s]**	**[s(a)s]**
s(a)g^-	**g^+(a)g^-**	**g^-(a)g^-**	**[s(a)g^-]**
s(a)g^+	**g^+(a)g^+**	**g^-(a)g^+**	**[s(a)g^+]**
s(a)s	**g^+(a)s**	**g^-(a)s**	**[s(a)s]**

Scheme 6.

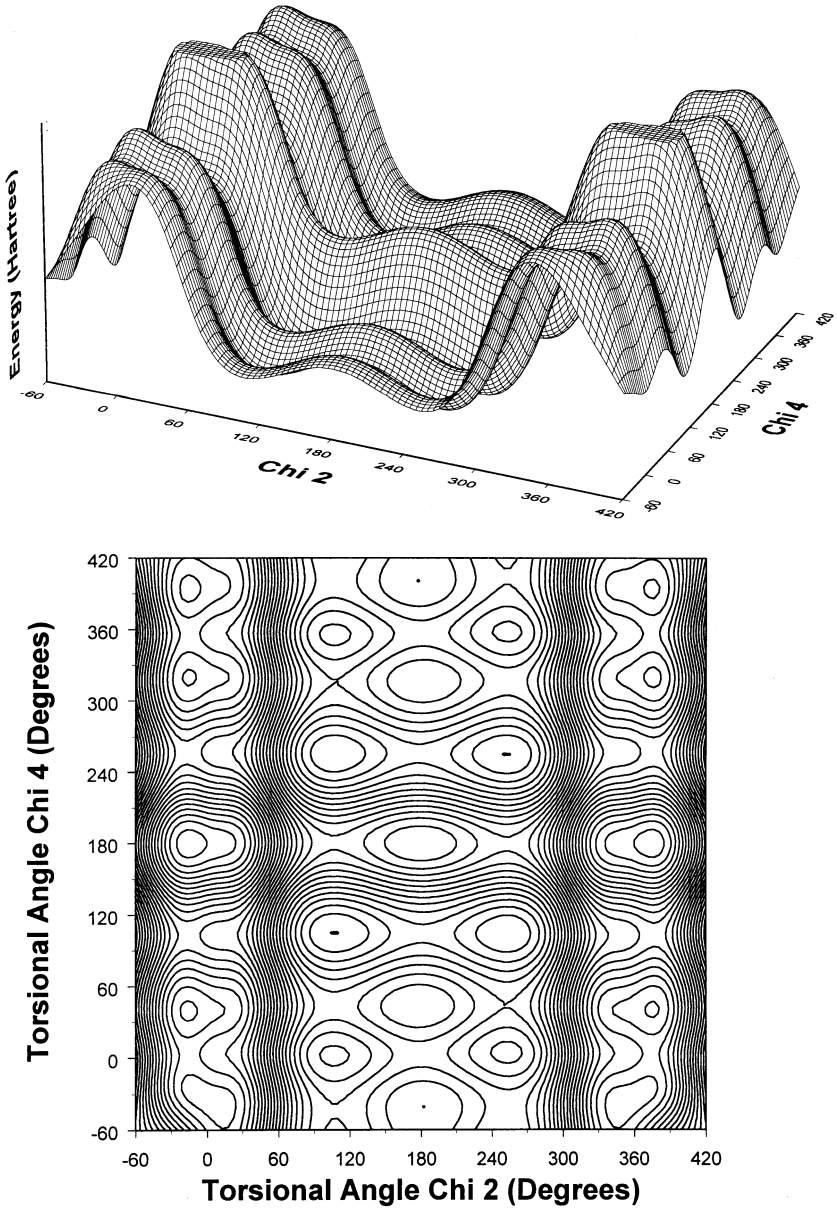

Fig. 3. All-*trans*-lycopene Model B PES, $E = f(\chi_2, \chi_4)$ at $\chi_3 =$ *anti* position. Top: Landscape representation. Bottom: Contour representation.

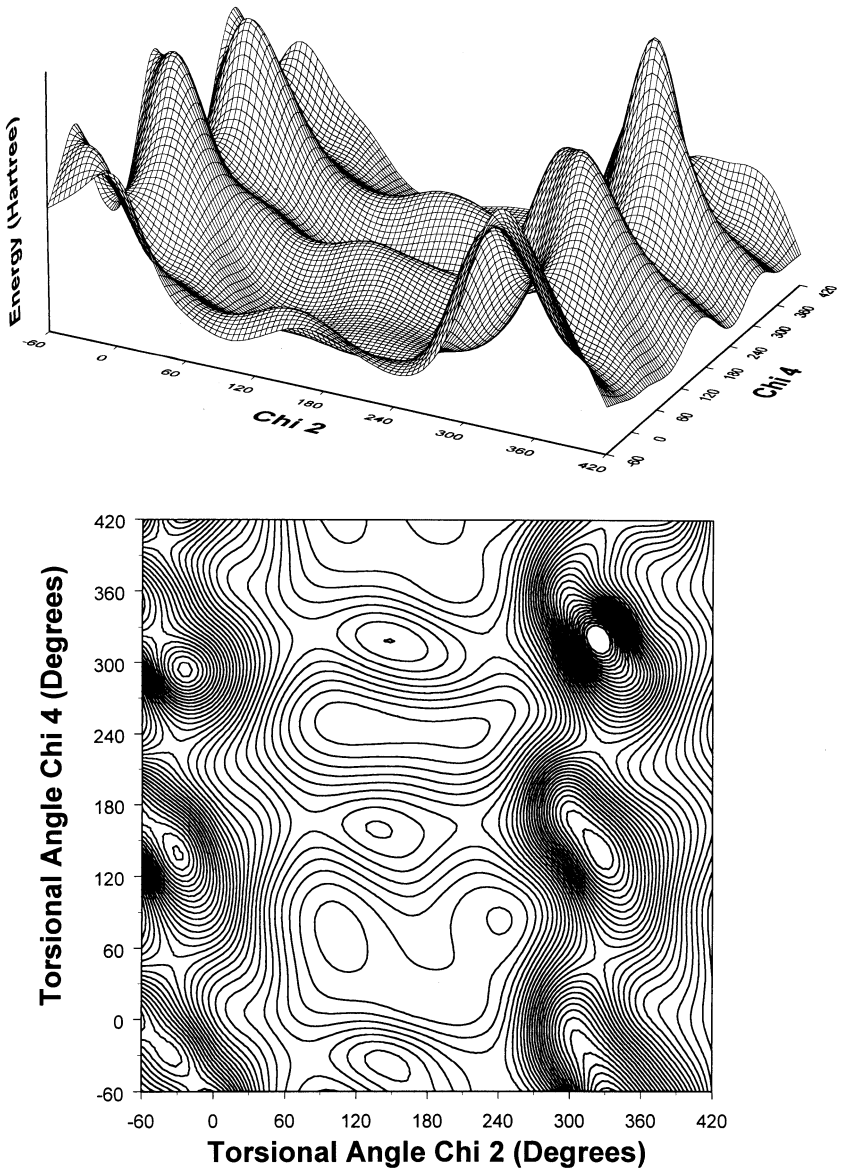

Fig. 4. All-*trans*-lycopene Model B PES, $E = f(\chi_2, \chi_4)$ at $\chi_3 = g^+$ position. Top: Landscape representation. Bottom: Contour representation.

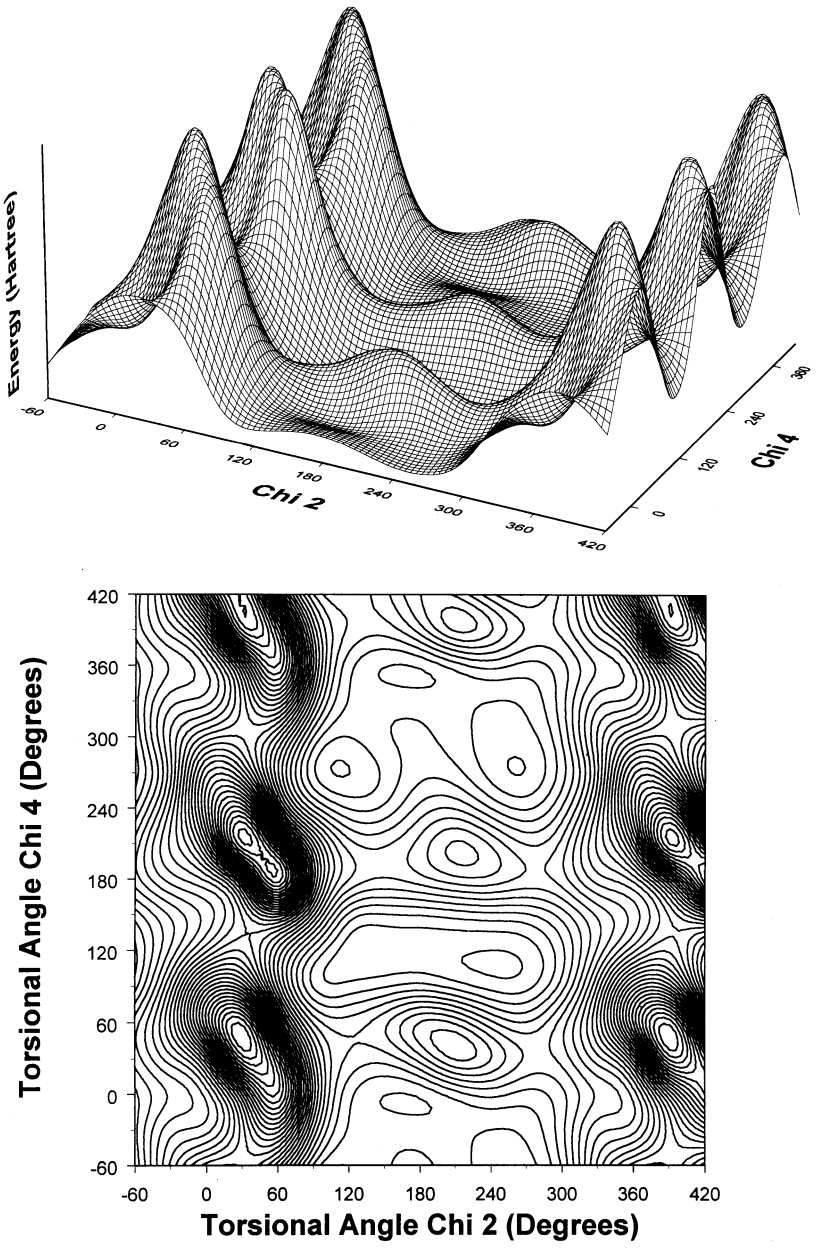

Fig. 5. All-*trans*-lycopene Model B PES, $E = f(\chi_2, \chi_4)$ at $\chi_3 = g^-$ position. Top: Landscape representation. Bottom: Contour representation.

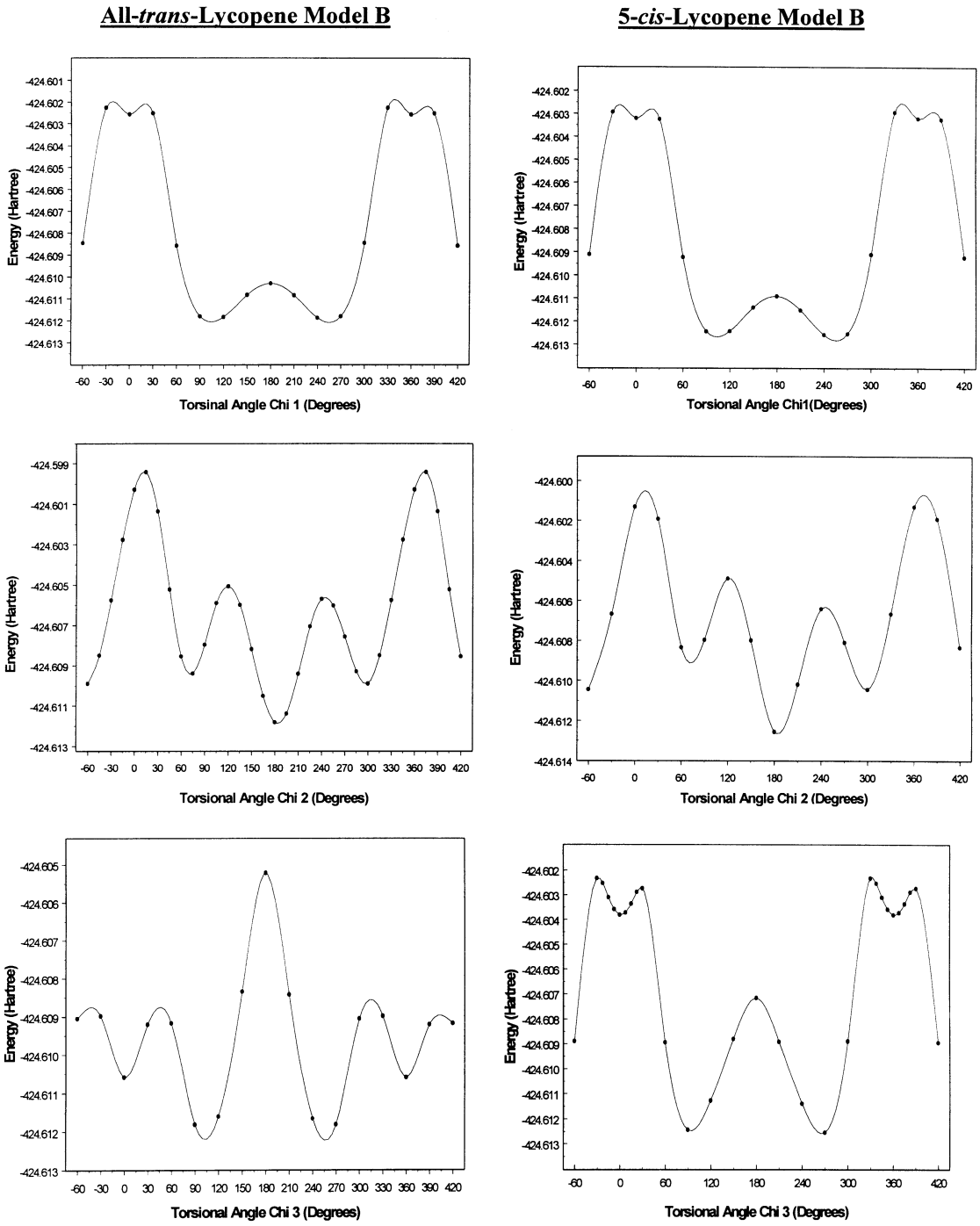

Fig. 6. Conformational PECs of lycopene tail-end Model B $E = g(\chi_2)$, $E = f(\chi_3)$, $E = f(\chi_4)$, according to Eq. (3a)–(3c), respectively. Left-hand side: all-*trans*-isomers. Right-hand side: 5-*cis*-isomers.

Table 1
Torsional angles of the optimized all-*trans* lycopene Model B conformers

Conformer			χ_1	χ_2	χ_3	χ_4	χ_5	χ_6	χ_7	χ_8	χ_9	χ_{10}
χ_2	χ_3	χ_4										
s	g^+	s	175.825	**8.219**	**73.456**	**−2.696**	178.530	179.109	−180.118	−1.567	155.285	179.822
s	g^+	g^+			**NOT**	**FOUND**		GOES	TO	$g^+g^+g^+$		
s	g^+	g^-			**NOT**	**FOUND**		GOES	TO	$g^+g^+g^-$		
g^+	g^+	s	180.620	**132.366**	**70.240**	**13.795**	178.533	180.080	−179.996	0.201	178.837	185.729
g^+	g^+	g^+	180.030	**99.689**	**59.014**	**79.958**	180.859	180.113	−180.005	0.247	179.439	172.338
g^+	g^+	g^-	180.584	**117.884**	**66.164**	**253.403**	179.837	180.202	−180.009	0.358	179.405	179.754
g^-	g^+	s	180.784	**−167.031**	**68.838**	**−0.291**	179.071	179.299	−180.081	−0.315	−179.499	
g^-	g^+	g^+	181.444	**−114.775**	**69.896**	**84.896**	181.140	180.181	−179.979	0.441	185.744	183.034
g^-	g^+	g^-	178.865	**−105.966**	**74.625**	**−98.969**	179.045	180.560	−179.990	0.277	176.476	−173.688
s	a	s	179.961	**−1.072**	**180.693**	**−0.550**	180.039	179.983	−180.001	0.016	179.745	179.679
s	a	g^+			**NOT**	**FOUND**		GOES	TO	g^+a g^+		
s	a	g^-			**NOT**	**FOUND**		GOES	TO	g^-a g^-		
g^+	a	s	180.835	**103.795**	**177.115**	**0.315**	179.902	179.969	−179.998	−0.037	179.214	180.142
g^+	a	g^+	181.065	**106.356**	**176.434**	**100.248**	181.363	180.202	−179.961	0.069	179.791	176.165
g^+	a	g^-	181.088	**104.305**	**177.254**	**−101.338**	178.588	179.917	−180.049	0.018	179.623	181.733
g^-	a	s	179.149	**−103.829**	**182.815**	**−0.257**	180.099	180.038	−180.001	0.083	180.774	179.863
g^-	a	g^+	178.912	**−104.659**	**182.837**	**101.431**	181.412	180.089	−179.959	0.006	180.344	178.335
g^-	a	g^-	178.956	**253.526**	**183.549**	**259.703**	178.637	179.818	−180.037	−0.067	180.284	183.768
s	g^-	s	184.130	**−8.143**	**−73.563**	**2.816**	181.474	180.903	180.116	1.777	155.308	−179.569
s	g^-	g^+			**NOT**	**FOUND**		GOES	TO	$g^-g^-g^+$		
s	g^-	g^-			**NOT**	**FOUND**		GOES	TO	$g^+g^-g^-$		
g^+	g^-	s	179.087	**167.376**	**−68.605**	**−0.093**	180.981	180.528	−179.921	0.683	179.219	180.034
g^+	g^-	g^+	181.140	**105.930**	**−74.655**	**98.949**	180.966	179.429	−180.010	−0.234	183.711	173.668
g^+	g^-	g^-	178.624	**114.557**	**−69.915**	**−84.922**	178.840	179.807	−180.014	−0.341	174.794	183.126
g^-	g^-	s	179.388	**−131.690**	**−70.369**	**−13.840**	181.446	179.922	−179.997	−0.460	180.771	174.221
g^-	g^-	g^+	179.402	**−117.654**	**−66.185**	**106.482**	180.151	179.865	−179.996	−0.269	180.616	179.818
g^-	g^-	g^-	−180.001	**−99.757**	**−58.865**	**−79.906**	179.135	179.874	−179.997	−0.381	180.530	187.383

angles (χ_8, χ_9 and χ_{10}) measure the spatial orientations of the three methyl groups of **III**.

The four central minima shown in Scheme 6 represent the two most stable conformations. They are pairwise equivalent, but they all practically have the same stability as shown in terms of ΔE (kcal mol^{-1}) in Scheme 7. The relative energies, together with the computed dipole moments, are summarized in Table 2.

In addition to the nine structures in Scheme 6,

$$g^+(a)g^- \quad g^-(a)g^- \longrightarrow 0.071 \quad 0.000$$

$$g^+(a)g^+ \quad g^-(a)g^+ \qquad\quad 0.000 \quad 0.071$$

Scheme 7.

where the central letter in parentheses represents *anti* orientation, (*a*), along χ_3, there are two additional sets of 9 structures; one set with (g^+) and the other with (g^-).

It is interesting to compare Figs. 4 and 5. They are centrosymmetric to each other through the fully symmetric (*a*, *a*, *a*) focal point, denoted as a heavy dot in Fig. 2. For this reason, the two sides of the 1D cross-section (**3b**), corresponding to the central left-hand side PEC, in Fig. 6, along with the heavy vertical line in Fig. 2, are not completely symmetrical. The g^+ and g^- minima differ slightly because the two surfaces at $\chi_2 = \chi_4 = 90°$, are not identical.

The centrosymmetric arrangement can also be seen from Scheme 8.

The discrepancies (1.063 versus 1.062 and 1.301 versus 1.302) are the result of regular optimization,

Table 2
Dipole moments, total energies and relative energies of the optimized all-*trans* lycopene Model B conformers

Conformer			Dipole	Energy (hartree)	ΔE (kcal mol^{-1})
χ_2	χ_3	χ_4			
s	g^+	s	0.7430	−424.6006056	7.381
s	g^+	g^+	Not found	GOES TO $g^+g^+g^+$	N/A
s	g^+	g^-	Not found	GOES TO $g^+g^+g^-$	N/A
g^+	g^+	s	0.8374	−424.6089342	2.155
g^+	g^+	g^+	1.0844	−424.6102939	1.301
g^+	g^+	g^-	0.6797	−424.6118287	0.338
g^-	g^+	s	0.6463	−424.6093099	1.919
g^-	g^+	g^+	0.8069	−424.6106742	1.063
g^-	g^+	g^-	0.5608	−424.6110997	0.796
s	a	s	0.8259	−424.604468	4.957
s	a	g^+	Not found	GOES TO g^+ag^+	N/A
s	a	g^-	Not found	GOES TO g^-ag^-	N/A
g^+	a	s	0.8872	−424.6108053	0.9805
***g*$^+$**	**a**	***g*$^+$**	**0.6568**	**−424.6123678**	**0.000**
g^+	*a*	g^-	*0.9860*	*−424.6122554*	*0.071*
g^-	a	s	0.8869	−424.6108055	0.980
g^-	*a*	g^+	*0.9861*	*−424.6122554*	*0.071*
***g*$^-$**	**a**	***g*$^-$**	**0.6571**	**−424.6123677**	**0.000**
s	g^-	s	0.7423	−424.6006059	7.3807
s	g^-	g^+	Not found	GOES TO $g^-g^-g^+$	N/A
s	g^-	g^-	Not found	GOES TO $g^+g^-g^-$	N/A
g^+	g^-	s	0.6492	−424.6093103	1.919
g^+	g^-	g^+	0.5602	−424.6110997	0.796
g^+	g^-	g^-	0.8070	−424.6106747	1.062
g^-	g^-	s	0.8412	−424.6089341	2.155
g^-	g^-	g^+	0.6794	−424.6118286	0.338
G^-	g^-	g^-	1.0843	−424.6102937	1.302

which are expected to disappear when the optimizations are performed to a tight convergence threshold.

4.1.2. The 5-cis-structure

The conformational PEHS (1) of three independent variables, shown schematically in Fig. 2 for the all-*trans*-isomer, is also valid for the 5-*cis*-isomer. In the case of the 5-*cis*-isomer, just as before, three PESs of two independent variables were generated for the $\chi_2 = \text{a}$, g^+ and g^- orientations. These are shown in Figs. 7–9, respectively. The 1D-scans produced three PECs (shown at the right-hand side of Fig. 6, Table 3).

The centrosymmetric arrangement can be seen, analogously to the all-*trans*-form, in the case for $\chi_2 =$ *anti*, in Scheme 9.

Similarly, the centrosymmetric character of the PEHS can be further demonstrated by comparing energies for the $\chi_3 = g^+$ and $\chi_3 = g^-$ cases. This is illustrated by Scheme 10.

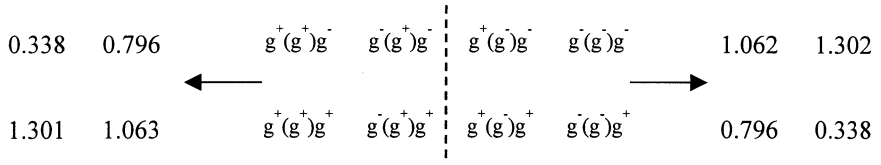

Scheme 8.

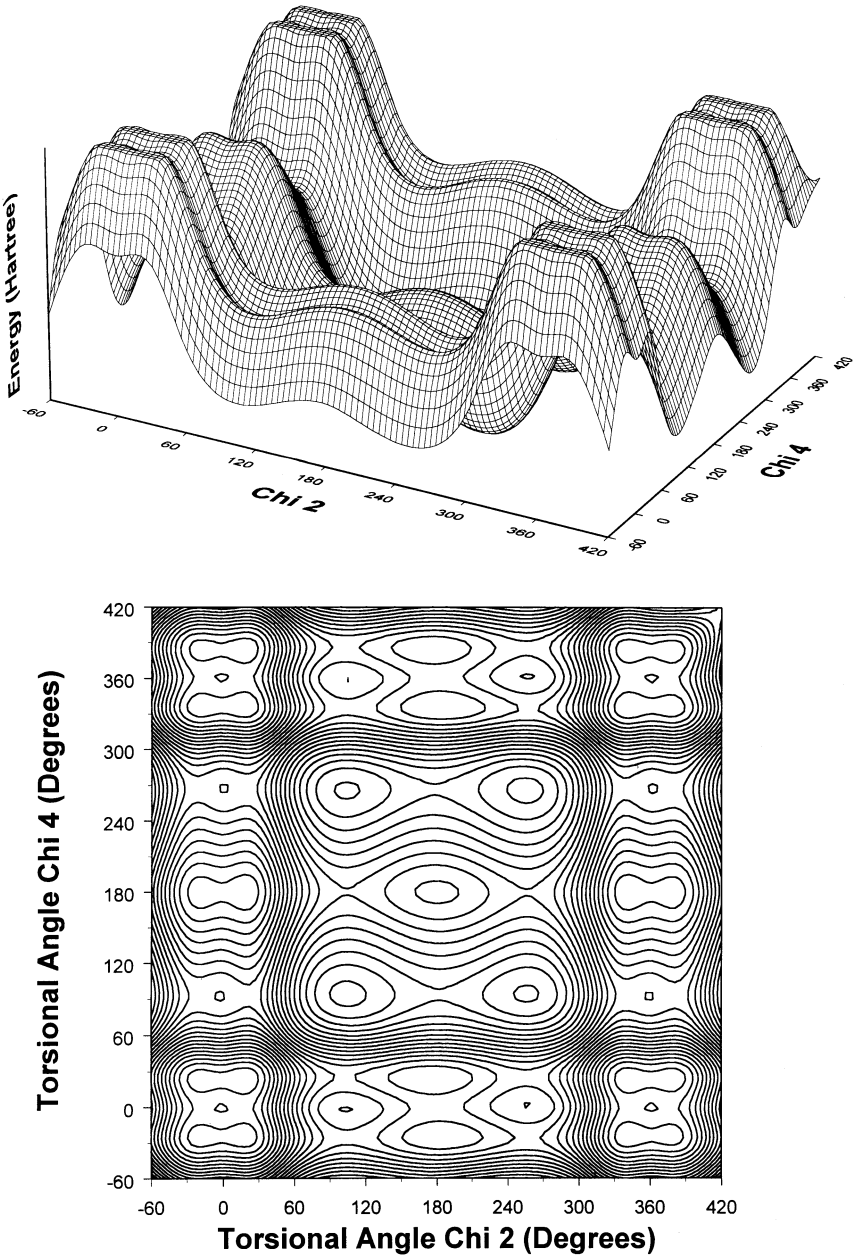

Fig. 7. The 5-*cis*-lycopene Model B PES, $E = f(\chi_2, \chi_4)$ at $\chi_3 =$ a conformation. Top: Landscape representation. Bottom: Contour representation.

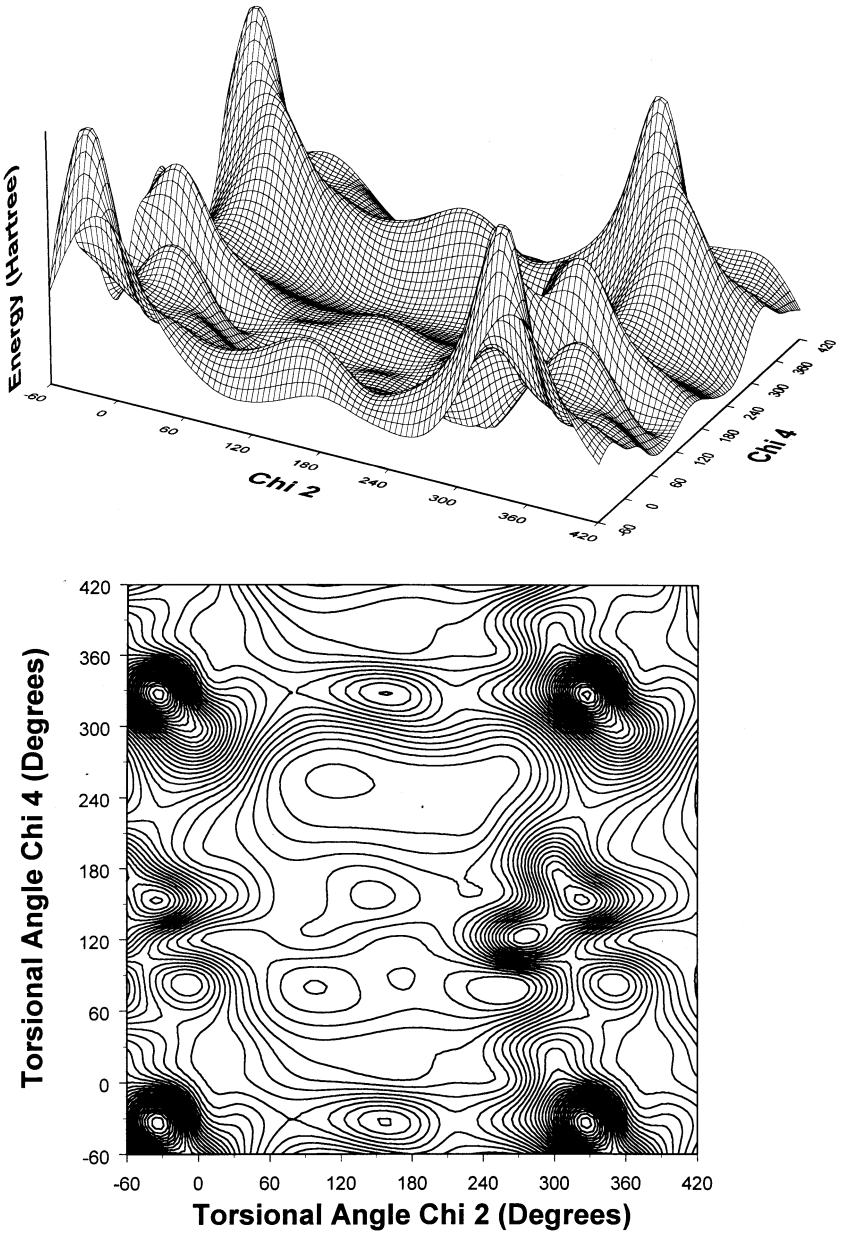

Fig. 8. The 5-*cis*-lycopene Model B PES, $E = f(\chi_2, \chi_4)$ at $\chi_3 = g^+$ conformation. Top: Landscape representation. Bottom: Contour representation.

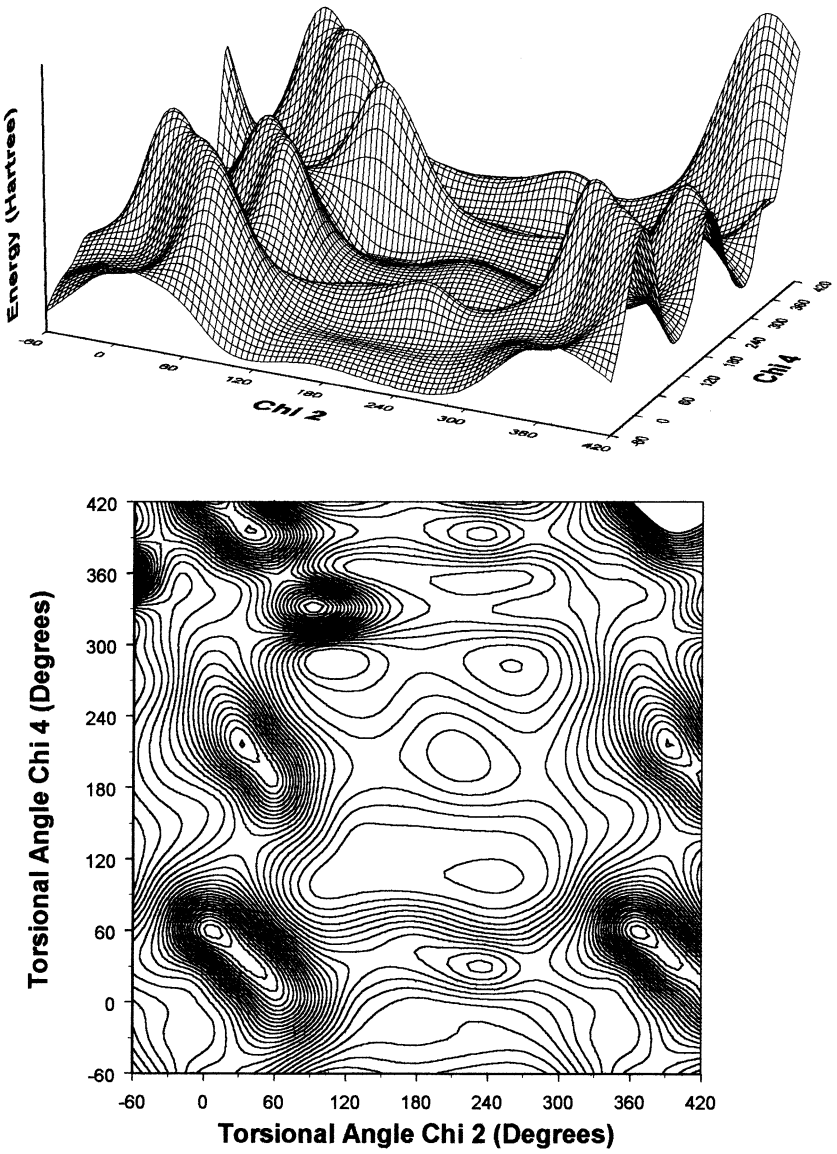

Fig. 9. The 5-*cis*-lycopene Model B PES, $E = f(\chi_2, \chi_4)$ at $\chi_3 = g^-$ conformation. Top: Landscape representation. Bottom: Contour representation.

Table 3
Torsional angles of the optimized 5-*cis* lycopene Model B conformers

Conformer			χ_1	χ_2	χ_3	χ_4	χ_5	χ_6	χ_7	χ_8	χ_9	χ_{10}
χ_2	χ_3	χ_4										
s	g^+	s	176.805	**−9.080**	**88.036**	**−8.820**	−4.471	170.478	−181.311	−1.685	163.845	178.980
s	g^+	g^+			**NOT**	**FOUND**		GOES	TO	s g^+s		
s	g^+	g^-			**NOT**	**FOUND**		GOES	TO	g^-a g^-		
g^+	g^+	s	180.452	**170.359**	**67.397**	**8.997**	−3.028	170.953	−180.864	−0.132	179.930	182.914
g^+	g^+	g^+	180.041	**99.783**	**58.797**	**79.371**	1.400	182.284	−179.580	0.255	179.460	175.630
g^+	g^+	g^-	180.717	**115.906**	**67.994**	**258.053**	0.596	181.810	−179.796	1.003	179.588	181.870
g^-	g^+	s			**NOT**	**FOUND**		GOES	TO	g^-a g^-		
g^-	g^+	g^+	181.120	**247.018**	**68**.508	**80.618**	0.963	182.754	−179.686	0.296	185.079	178.317
g^-	g^+	g^-	178.111	**−105.361**	**75.434**	**−100.127**	−0.038	181.286	−180.039	−2.349	−182.219	−177.214
s	a	s			**NOT**	**FOUND**		GOES	TO	g^+a g^+		
s	a	g^+			**NOT**	**FOUND**		GOES	TO	g^+a g^+		
s	a	g^-			**NOT**	**FOUND**		GOES	TO	g^+a g^+		
g^+	a	s	180.860	**102.780**	**174.547**	**4.853**	0.122	180.257	−179.872	−0.077	179.099	181.457
g^+	a	g^+	181.099	**104.375**	**175.566**	**91.422**	1.315	181.324	−179.966	−0.001	179.400	176.023
g^+	a	g^-	181.052	**103.802**	**179.675**	**−91.919**	−1.255	179.048	−180.005	0.009	179.441	183.829
g^-	a	s	179.155	**−102.865**	**185.316**	**−4.575**	−0.114	179.658	−180.125	0.129	181.131	178.668
g^-	a	g^+	178.939	**−103.962**	**180.368**	**91.951**	1.255	180.915	−179.994	0.014	180.608	176.131
g^-	a	g^-	178.916	**−104.231**	**184.418**	**−91.459**	−1.320	178.750	−180.030	−0.021	180.516	184.011
s	g^-	s	183.218	**9.068**	**−88.104**	**8.891**	4.444	189.461	181.309	1.637	196.198	181.053
s	g^-	g^+			**NOT**	**FOUND**		GOES	TO	g^- g^- g^+		
s	g^-	g^-			**NOT**	**FOUND**		GOES	TO	g^- g^- g^-		
g^+	g^-	s			**NOT**	**FOUND**		GOES	TO	g^- g^- g^+		
g^+	g^-	g^+	181.885	**105.325**	**−75.373**	**100.166**	0.061	178.649	−179.960	−2.389	181.962	176.975
g^+	g^-	g^-	178.875	**113.110**	**−68.478**	**−80.610**	−0.968	177.325	−180.320	−0.360	174.822	181.661
g^-	g^-	s	179.535	**−170.224**	**−67.490**	**−8.822**	3.006	188.995	−179.135	0.295	180.655	177.220
g^-	g^-	g^+	179.289	**−115.815**	**−68.005**	**101.908**	−0.598	178.149	−180.201	−0.988	180.411	178.083
g^-	g^-	g^-	179.946	**−99.765**	**−58.836**	**−79.395**	−1.406	177.812	−180.418	−0.159	180.651	184.473

The optimized torsional angles are summarized in Table 4 and the computed properties are given in Table 4.

4.2. Molecular configurations

It is of considerable interest to optimize the fully symmetrical *a*,*a*,*a* ($\chi_2 = \chi_3 = \chi_4 = 180°$) conformation. This is done for both the all-*trans* and the 5-*cis* structures, in two steps. First, these three dihedral angles were kept frozen and then subsequently relaxed. In addition to the optimized torsional angles (Table 5), the energies and the imaginary frequencies (Table 6) were also tabulated. These fully symmetric points (marked as a solid dot at the centre of Fig. 2) are second order saddle points. All these indicate that neither the all-*trans*, nor the 5-*cis* isomers are ever fully symmetric. Consequently, neither the all-*trans* nor the 5-*cis* isomers are planar.

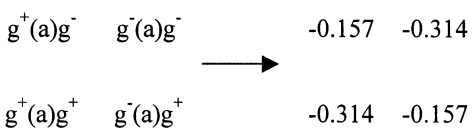

Scheme 9.

It is interesting to compare the relative stability of the all-*trans*- and the 5-*cis*-isomers. A graphical comparison of the relative energies given in Tables 2 and 4, is shown in Fig. 10. Intuitively, one would have guessed that all 5-*cis*-conformers have to be of higher energy than their corresponding all-*trans*-conformers. However, this is not the case.

Only four conformers of the 5-*cis*-isomer (sg^+s,

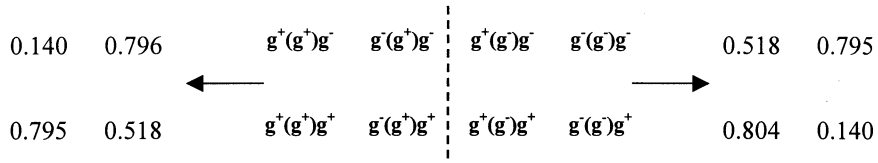

Scheme 10.

Table 4
Dipole moments, total energies and relative energies of the optimized 5-*cis* lycopene Model B conformers

Conformer			Dipole	Energy (hartree)	ΔE (kcal mol^{-1})
χ_2	χ_3	χ_4			
s	g^+	s	0.8089	− 424.5945699	11.168
s	g^+	g^+	NOT FOUND	GOES TO s g^+s	N/A
s	g^+	g^-	NOT FOUND	GOES TO g^-a g^-	N/A
g^+	g^+	s	0.8657	− 424.6023298	6.2989
g^+	g^+	g^+	1.0293	− 424.6111013	0.7947
g^+	g^+	g^-	0.7313	− 424.6121441	0.1404
g^-	g^+	s	NOT FOUND	GOES TO g^+a g^+	N/A
g^-	g^+	g^+	0.7078	− 424.6115428	0.5177
g^-	g^+	g^-	0.5608	− 424.6110997	0.7957
s	a	s	NOT FOUND	GOES TO g^+a g^+	N/A
s	a	g^+	NOT FOUND	GOES TO g^+a g^+	N/A
s	a	g^-	NOT FOUND	GOES TO g^- g^- g^+	N/A
g^+	a	s	0.9719	− 424.6040333	5.2300
g^+	**a**	**g^+**	**0.6513**	**− 424.6128689**	**− 0.3140**
g^+	**a**	**g^-**	**0.9975**	**− 424.6126178**	**− 0.1570**
g^-	a	s	0.9716	− 424.6040331	5.2301
g^-	**a**	**g^+**	**0.9976**	**− 424.6126178**	**− 0.1570**
g^-	**a**	**g^-**	**0.6515**	**− 424.6128689**	**− 0.3140**
s	g^-	s	0.8091	− 424.5945699	11.1680
s	g^-	g^+	NOT FOUND	GOES TO g^- g^- g^+	N/A
s	g^-	g^-	NOT FOUND	GOES TO g^- g^- g^-	N/A
g^+	g^-	s	NOT FOUND	GOES TO g^- g^- g^+	N/A
g^+	g^-	g^+	0.6145	− 424.6110874	0.8035
g^+	g^-	g^-	0.7079	− 424.6115427	0.5178
g^-	g^-	s	0.8654	− 424.6023291	6.2994
g^-	g^-	g^+	0.7314	− 424.6121441	0.1404
g^-	g^-	g^-	1.0296	− 424.6111013	0.7947

Table 5
Torsional angles of the symmetric second order TS lycopene Model B isomers

Conformer	χ_1	χ_2	χ_3	χ_4	χ_5	χ_6	χ_7	χ_8	χ_9	χ_{10}
Trans	179.973	**180.000**	**180.000**	**180.000**	180.000	179.996	180.000	0.181	180.124	180.121
5-Cis	180.001	**180.000**	**180.000**	**180.000**	−0.0008	180.001	−179.999	0.025	180.005	179.981

Table 6
Imaginary frequencies, dipole moments, total energies and relative energies of the symmetric second order TS of lycopene Model B isomers

Conformer	Imaginary frequencies (cm^{-1})		Dipole	Energy (hartree)	ΔE (kcal $mol^{-}1$)
Trans	115.5i	51.0i	1.1343	−424.6036305	5.4827
5-Cis	77.1i	19.6i	1.0753	−424.6055073	4.305

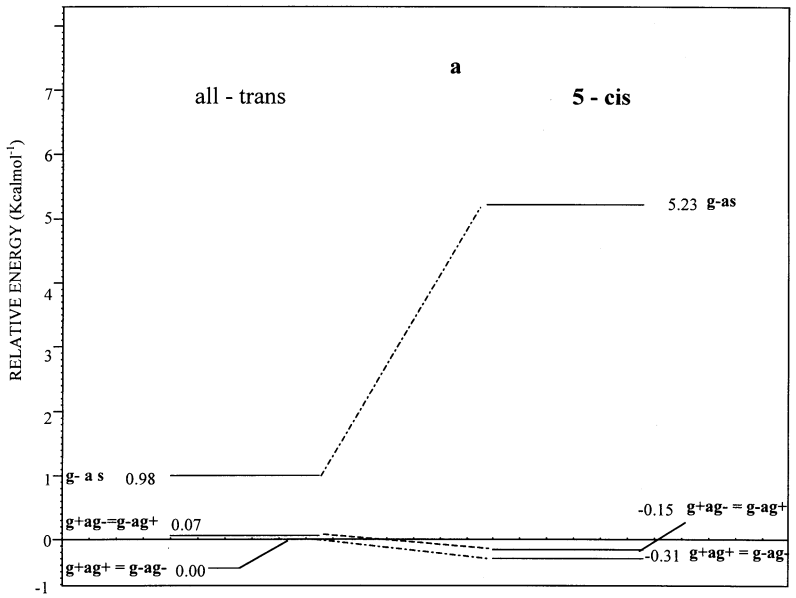

Fig. 10. Relative energy of the all-*trans* and 5-*cis*-isomers of lycopene Model B at the $\chi_3 =$ a conformation.

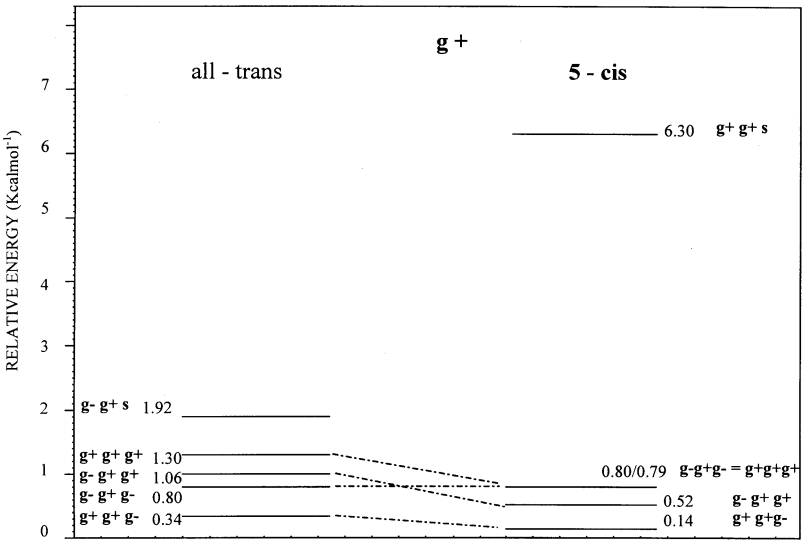

Fig. 11. Relative energy of the all-*trans* and 5-*cis*-isomers of lycopene Model B at the $\chi_3 = g^-$ conformation.

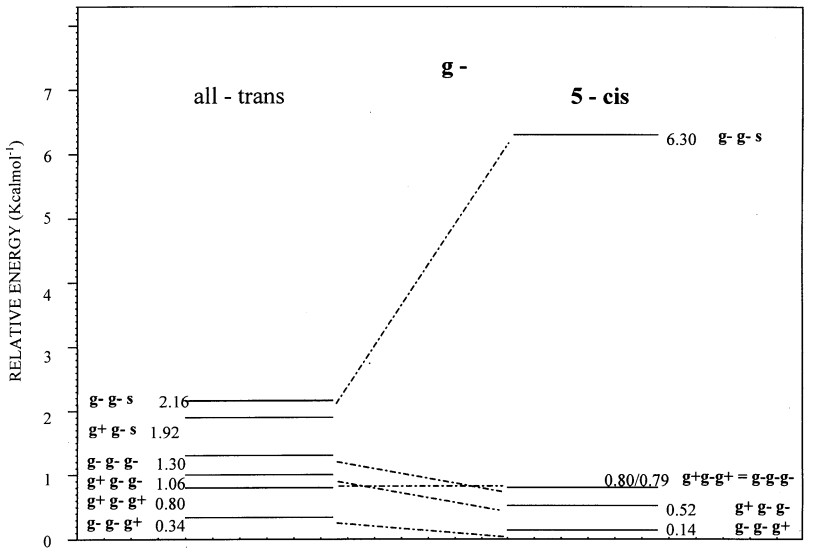

Fig. 12. Relative energy of the all-*trans* and 5-*cis*-isomers of lycopene Model B at the $\chi_3 = g^+$ conformation.

g^-g^+s, g^-as, g^-g^-s) had higher energy than the corresponding all-*trans* isomer. Two conformers ($g^-g^+g^-$ and $g^+g^-g^+$) had practically the same energies, while in the case of the other conformers, the 5-*cis*-isomers were slightly more stable, than their corresponding all-*trans*-isomers (Figs. 11 and 12).

5. Conclusions

Epidemiological studies have supported the hypothesis that consumption of heat processed tomatoes, such as in the Mediterranean diet, may reduce the risk of coronary heart disease by preventing the oxidation of the low-density lipoprotein [1,2]. Giovannucci et al. have also suggested that only the intake of processed tomato products was related to reduced risk of prostate cancer probably because of their high *cis* isomer content of lycopene [21]. The observation that high concentration of *cis* isomers are present in human serum and prostate tissue, also suggests that *cis* isomers might be biologically more active than the all-*trans* isomer.

In contrast to previous results [22], according to which the *cis*-isomer is less stable than the corresponding *trans*-isomer, the present study suggests at least the 5-*cis*-isomer is more stable than the all-*trans*-isomer. Such stability may be due to the favourable Type A′ 1,4-interaction (Scheme 4). The conformational study revealed that the fully planar structure of lycopene Model B, is a second-order saddle point. Such fully symmetric (i.e. planar) structure of lycopene would be expected to become a fourth-order critical point on its PEHS, because there are two negative eigenvalues at both ends (χ_2, χ_4 as well as $\chi_{2'}$, $\chi_{4'}$).

Acknowledgements

One of the authors (GAC) wishes to thank Graydon Hoare (graydon@pobox.com) for database management, network support, software and distributive processing development. A special thanks is also extended to Andrew M. Chasse for his continuing and ongoing development of novel scripting and coding techniques indirectly bringing about a reduction in the necessary number of CPU cycles for each computations.

References

[1] A.V. Rao, S. Agarwal, Nutr. Res. 19 (1999) 305–323.
[2] S.K. Clinton, Nutr. Res. 56 (1998) 35–51.
[3] E. Giovannucci, J. Natl Cancer Ins. 91 (1999) 317–331.

[4] R. Willstätter, H.H. Escher, Z. Physiol. Chem. 64 (1910) 47–61.
[5] P. Karrer, R.P. Widmer, Helv. Chim. Acta 11 (1928) 751–752.
[6] P. Karrer, A. Helfenstein, R.P. Widmer, Helv. Chim. Acta 11 (1928) 1201–1209.
[7] P. Karrer, W.E. Bachmann, Helv. Chim. Acta 12 (1929) 285–291.
[8] P. Karrer, A. Helfenstein, H. Wehrli, A.P. Wettstein, Helv. Chim. Acta. 13 (1930) 1084–1099.
[9] L. Zechmeister, A.L. LeRosen, W.A. Schroeder, A. Polgar, L. Pauling, J. Am. Chem. Soc. 65 (1943) 1940–1955.
[10] L. Zechmeister, P. Tuzson, Nature 141 (1938) 249–250.
[11] A. Polgar, L. Zechmeister, J. Am. Chem. Soc. 64 (1942) 1856–1861.
[12] L. Zechmeister, A. Polgar, J. Am. Chem. Soc. 65 (1943) 1522–1528.
[13] L. Zechmeister, R.B. Escue, J. Am. Chem. Soc. 66 (1944) 322–330.
[14] L. Pauling, Fortschr. Chem. Organ. Naturstoffe. 3 (1939) 203–235.
[15] C. Sterling, Acta Crystallogr. 17 (1964) 1224–1228.
[16] M.O. Senge, H. Hope, K.M. Smith, Z. Naturforsch. Teil C. 47 (1992) 474–480.
[17] M.L. Nguyen, S.J. Schwartz, Food Technol. 53 (1999) 38–45.
[18] S.K. Clinton, C. Emenhiser, S.J. Schwartz, D.G. Bostwick, A.W. Williams, B.J. Moore, J.W. Erdman Jr., Cancer Epidemiol Biomarkers Prev. 5 (1996) 823–833.
[19] Ö. Farkas, S.J. Salpietro, P. Császár, I.G. Csizmadia, J. Mol. Struct. (Theochem) 367 (1996) 25–31.
[20] M.J. Frisch, G.W. Trucks, H.B. Schlegel, P.M.W. Gill, B.G. Johnson, M.A. Robb, J.R. Cheeseman, T. Keith, G.A. Petersson, J.A. Montgomery, K. Raghavachari, M.A. Al-Laham, V.G. Zakrzewski, J.V. Ortiz, J.B. Foresman, J. Cioslowski, B.B. Stefanov, A. Nanayakkara, M. Challacombe, C.Y. Peng, P.Y. Ayala, W. Chen, M.W. Wong, J.L. Andres, E.S. Replogle, R. Gomperts, R.L. Martin, D.J. Fox, J.S. Binkley, D.J. Defrees, J. Baker, J.P. Stewart, M. Head-Gordon, C. Gonzalez, J.A. Pople, Gaussian, Inc., Pittsburgh PA, 1995.
[21] E. Giovannucci, A. Ascherio, E.B. Rimm, M.J. Stampfer, G.A. Colditz, W.C. Willett, J. Natl. Cancer Inst. 87 (1995) 1767–1776.
[22] M.A. Berg, G.A. Chasse, E. Deretey, A.K. Füzéry, B.M. Fung, D.Y.K. Fung, H. Henry-Riyad, A.C. Lin, M.L. Mak, A. Mantas, M. Patel, I.V. Repyakh, M. Staikova, S.J. Salpietro, Ting-Hua Tang, J.C. Vank, András Perczel, Ödön Farkas, Ladislaus L. Torday, Zoltán Székely, Imre G. Csizmadia, J. Mol. Struct. (Theochem) 500 (2000) 5–58.